

Suppression of matching field effects by splay and pinning energy dispersion in $\text{YBa}_2\text{Cu}_3\text{O}_7$ with columnar defects

D. Niebieskikwiat, A. Silhanek, L. Civale, and G. Nieva
*Comisión Nacional de Energía Atómica-Centro Atómico Bariloche
 and Instituto Balseiro, 8400 Bariloche, Argentina*

P. Levy

Comisión Nacional de Energía Atómica-Departamento de Física, Av. Libertador 8250, 1429 Buenos Aires, Argentina

L. Krusin-Elbaum

IBM T. J. Watson Research Center, Yorktown Heights, New York 10598

We report measurements of the irreversible magnetization M_i of a large number of $\text{YBa}_2\text{Cu}_3\text{O}_7$ single crystals with columnar defects (CD). Some of them exhibit a maximum in M_i when the density of vortices equals the density of tracks, at temperatures above 40K. We show that the observation of these *matching field effects* is constrained to those crystals where the orientational and pinning energy dispersion of the CD system lies below a certain threshold. The amount of such dispersion is determined by the mass and energy of the irradiation ions, and by the crystal thickness. Time relaxation measurements show that the matching effects are associated with a reduction of the creep rate, and occur deep into the collective pinning regime.

I. INTRODUCTION

Vortex dynamics in high temperature superconductors (HTSC) with columnar defects (CD) depends on a number of variables such as the density and angular distribution of the CD, the intensity and orientation of the applied magnetic field \mathbf{H} , and the temperature T . The complexity of these systems results in the existence of a rich variety of pinning and creep regimes.^{1,2}

The simplest case to model^{1,2} is that of identical and perfectly parallel CD and \mathbf{H} parallel to them. At low T , and for H much smaller than the *matching field* B_Φ (the dose-equivalent field at which the densities of vortices and CD are the same), vortex-vortex interactions can be neglected and each vortex is individually pinned to an individual track. For $H > B_\Phi$ there are more vortices than defects and pinning becomes collective. As T increases, thermal fluctuations progressively reduce the effective pinning energy of the CD, thus the vortex-vortex interactions turn more significant and the boundary separating the individual from the collective regimes, the so-called *accommodation field* $B_a(T)$, decreases.³

An interesting situation occurs for $H \sim B_\Phi$. At low T a Mott insulator phase is predicted.^{1,2} The fingerprint of this phase is the infinite elastic compression modulus C_{11} , that results in a constant induction field B (fixed density of vortices) over a finite range of H . The dynamics is also influenced by the matching condition. As all the CD are occupied, a pinned vortex has no energetically convenient places to jump into, with the consequent reduction of the creep rate. The Mott phase has indeed been observed in time relaxation experiments at very low T , by

Beauchamp *et al.*⁴ in $\text{YBa}_2\text{Cu}_3\text{O}_7$ (YBCO) crystals and by Nowak *et al.*⁵ in Tl:2201 crystals.

At high T the wandering of the vortex lines precludes their localization into individual CD. Although this effect should inhibit the appearance of the Mott insulator phase,^{1,2} some reduction in the vortex mobility is still expected due to the absence of empty tracks. However, many studies of vortex pinning by CD in HTSC have failed to show any evidence of *matching effects* at high temperatures. This status was modified by a recent study performed by Mazilu *et al.*⁶ on YBCO thick films (thickness $\delta \sim 1\mu\text{m}$) with CD $\parallel c$ -axis. For $\mathbf{H} \parallel \text{CD}$, they observed that the transport critical current had a broad peak at $H \sim B_\Phi$, at temperatures as high as 75K.

In this work we report the observation of matching effects due to CD introduced by heavy ion irradiation in YBCO single crystals. We observe such effects at high temperatures, deep into the collective pinning regime. For crystals with CD in different crystallographic orientations, we find that for $\mathbf{H} \parallel \text{tracks}$, the irreversible magnetization $M_i(H)$ exhibits a local maximum at $H \sim B_\Phi$. That maximum is associated with a local minimum in the normalized time relaxation rate $S = -d(\ln M_i)/d(\ln t)$. We show that the appearance of these matching effects requires a narrow angular distribution (small splay) and a small pinning energy dispersion of the CD. These conditions impose a maximum track length (given by the sample thickness and the irradiation angle) that depends on the mass and energy of the irradiation ions.

II. EXPERIMENTAL

We have observed matching effects in four YBCO single crystals. For comparison, we show analogous measurements in several other YBCO crystals that do not exhibit such effects. A group of crystals was grown at the Centro Atómico Bariloche⁷ and was irradiated with 300MeV Au^{24+} ions at the Tandem facility in Buenos Aires, Argentina.⁸ Another group was grown at the T.J. Watson Research Center of IBM.⁹ Some of them were irradiated¹⁰ with 1.08GeV Au^{23+} at the TASCC facility in Chalk River Laboratories, Canada, and the rest¹¹ with 580MeV Sn^{30+} at the Holifield accelerator, Oak Ridge, USA. The crystal thicknesses δ , the matching fields B_Φ and the angle Θ_D between the incident beam and the c -axis are summarized in table I.

Measurements of dc magnetization were made in two commercial superconducting quantum interference device (SQUID) magnetometers, both equipped with 50kOe magnets. The irreversible magnetization M_i (proportional to the persistent current density J via the critical state model) was determined from $M(H)$ loops. The magnetic field was always applied parallel to the irradiation direction. In crystals where $\Theta_D \neq 0$, both components of $\mathbf{M}_i(H)$ were recorded using the two sets of pick up coils (longitudinal and transverse), and the data were processed in the way previously described.¹² Relaxation measurements of M_i were performed on the field decreasing branch of the hysteresis loop over periods of 2 hours.

III. RESULTS

A. Sample thickness influence on matching effects

In Fig. 1(a) we show M_i as a function of H for crystal A1 at several temperatures between 40K and 75K , for $\mathbf{H} \parallel$ tracks ($\Theta_D \approx 57^\circ$). These curves show a clear maximum at fields $H_m(T)$ close to B_Φ . This *matching effect* is very similar to that found by Mazilu *et al.*⁶ in transport measurements of critical current in YBCO thick films with $\mathbf{H} \parallel \text{CD} \parallel c$ -axis. The temperature dependence of H_m/B_Φ for both our crystal and a thick film with $B_\Phi \sim 3.9T$, taken from Ref. 6, is shown in Fig. 2. Several features reinforce the similarity between the results of that study and our data. First, at the lowest temperatures the maximum occurs slightly above the matching field B_Φ . Second, the field H_m slowly decreases with increasing T . Third, the maximum disappears at low temperatures, below 40K in our case.

Many measurements of M_i in YBCO crystals with CD, in the same field and temperature ranges of Fig. 1, can be found in the literature. Usually, the maximum shown in Fig. 1(a) is not observed. The question is why these matching effects are visible in some cases and not in others. Clearly, it is not due to a structural characteristic

of the thick films, as they are also visible in a crystal. The orientation of the CD is not relevant either. A distinctive characteristic of crystal A1 is that it is unusually thin, $\delta \approx 4.1\mu\text{m}$. The thick films measured by Mazilu *et al.*⁶ are of course even thinner, $\delta \sim 1\mu\text{m}$. In contrast, most YBCO crystals with CD reported in previous studies have typical thicknesses between $10\mu\text{m}$ and $30\mu\text{m}$. This observation suggests that the appearance of matching effects may be restricted to thin samples.

To test this hypothesis, we have collected $M_i(H)$ data for a representative group of 13 additional crystals. We have included crystals irradiated with ions of different mass and energy, at a variety of B_Φ and Θ_D , as indicated in table I. In all cases $\mathbf{H} \parallel \text{CD}$. Figure 3 shows $M_i(H)$ curves for 10 crystals. None of them show any evidence of matching effects. For clarity only data at $T = 60\text{K}$ are shown, but in all cases the maximum is also absent at other temperatures within the range $40\text{K} \leq T \leq 80\text{K}$. In contrast, the $M_i(H)$ curves of crystals B1 and B2, shown in Figs. 4(a) and (b) respectively, do exhibit a clear maximum in the vicinity of B_Φ . Again in these two crystals H_m decreases slowly with temperature. Finally, in crystal B3, shown in Fig. 4(c), a small structure in $M_i(H)$ near B_Φ just suggests the existence of minor matching effects. In the three crystals (B1, B2 and B3) the matching effects disappear below 40K .

Inspection of Figs. 1 and 4 show that, at $T \sim 40\text{K}$, the ratio H_m/B_Φ is ~ 1.1 for crystal A1, while it is only ~ 0.75 for B1 and ~ 0.85 for B2. This difference may be due to clustering of the tracks.³ As B_Φ increases, also does the probability that two or more CD are so close together that they act as a single one. The result is an “effective” matching field lower than the nominal B_Φ . For crystal B1, the effective tracks’ density was found³ to be $\sim 0.7B_\Phi$, while for a crystal with a dose similar to A1 the result was $\sim 0.9B_\Phi$. Thus, there is a reasonable agreement between both results, indicating that H_m is in all cases slightly higher than the *effective* matching field.

To some extent data in Figs. 3 and 4 reinforce the idea that matching effects are associated with thin samples, as crystals B1 and B2 are among the thinnest in the group. However, it is clear that the correlation is far from perfect; crystals A2, A3 and B5, which are as thin as B1 and B2 or even thinner, show no maximum at B_Φ . Another exception is crystal B3, which is rather thick and shows at least a hint of the effect.

The simplest connection between sample thickness and matching effects could be related to the inhomogeneity of the internal field B . It is natural to expect that matching effects should be visible over a finite field range ΔB_{me} around B_Φ . On the other hand, in the critical state of a thin superconducting slab in a transverse field configuration, B has a total variation¹³ $\Delta B \sim (4\pi/c)J\delta/2$ between the center and the border of the sample. Therefore, the required conditions for observation of matching effects can be satisfied over the whole sample only if $\Delta B < \Delta B_{me}$. Otherwise, the maximum in $M_i(H)$ will be washed away.

We can estimate ΔB at $T = 60K$ and in the proximity of B_Φ for all the crystals. It ranges from $\Delta B \sim 0.12kG$ for crystal A1 to $\Delta B \sim 0.6kG$ for crystals C4 and C5. An estimate of ΔB_{me} is given by the width of the maximum in $M_i(H)$. From Figs. 1 and 4 we see that ΔB_{me} is similar in crystals A1, B1 and B2, and in all cases it is well above $10kG$. Thus, we conclude that even in the thickest crystals $\Delta B \ll \Delta B_{me}$, so the inhomogeneity in the internal field cannot be the reason for the absence of matching effects.

B. Energy and angular dispersion of the CD

Sample thickness influences pinning by CD in a more indirect way, as it affects the morphology and the disorder of the tracks. When a sample is irradiated, the heavy ions arrive to the surface with an extremely narrow distribution of energy and orientations. Thus, all the CD are initially identical and exactly parallel. But as they penetrate deeper into the material, their energy decreases rapidly due to the very large electronic stopping power. As a result, the diameter of the tracks initially decreases as a function of depth, then becomes oscillatory and eventually the tracks turn discontinuous as the ions approach their penetration range.¹⁴ Consequently, there is a certain dispersion in the pinning energy of the CD. In addition, the scattering with the atomic cores of the material (associated with the small but nonzero nuclear stopping power) deviates the incident ions from the original direction. The cumulative effect of these nuclear interactions produces^{10,15} an angular dispersion (splay) of the tracks that grows with depth, first slowly and then dramatically near the ion penetration range. These effects have been clearly demonstrated in several transmission electron microscopy (TEM) studies.^{10,14,15}

The above considerations indicate that, in all cases, real CD introduced by swift heavy-ion irradiation contain some amount of splay and pinning energy dispersion. For given irradiation conditions, the distributions of pinning energies and orientations are wider for thicker samples. We will now argue that this larger dispersion in the tracks precludes the observation of matching effects in thick crystals.

At this point we need a more quantitative measure of the amount of disorder in the system of CD. We first note that the relevant parameter is not the thickness of the crystal, but rather the length of the tracks, $l_D = \delta / \cos \Theta_D$, which are also listed in table I. We see that the shorter $l_D \sim 7.5\mu m$ still corresponds to crystal A1. The l_D of crystals B1 and B2 still rank among the shortest, and the discrepancy of B5 is solved, as due to the large Θ_D we have a large $l_D \sim 27\mu m$ for this case.

Splay and energy dispersion as a function of depth depend in a complex way on the ion mass and initial energy.^{14,15} We look for a simpler description where disorder is characterized by a single parameter. In Ref. 10

the median radial angle α_{SP} of the angular distribution of CD was determined as a function of depth in YBCO crystals, for CD produced by $1.08GeV Au^{23+}$ and $580MeV Sn^{30+}$. The determination was based on TRIM numerical calculations that coincided very well with direct measures of α_{SP} at selected depths from TEM images. We have repeated those TRIM Monte Carlo calculations and extended them to the $300MeV Au^{24+}$ case. If our assumption is correct, matching effects will be erased if α_{SP} is large enough. Thus, to quantify the splay of the CD we have chosen the largest α_{SP} in each crystal, which occurs at the back end of the tracks.

In Fig. 5 we plotted α_{SP} at l_D for all our crystals. Note that the data points are separated in 3 groups corresponding to each type of irradiation. An additional data point corresponding to the thick films of Ref. 6 is also included. It is unmistakably clear that there is a threshold value of $\alpha_{SP}(l_D) \approx 3.4^\circ$ above which the matching effects disappear. All samples with $\alpha_{SP}(l_D)$ well below the threshold (B1, B2 and the thick films) exhibit clear matching effects. None of the nine crystals with $\alpha_{SP}(l_D)$ well above the threshold show any hint of it. Finally we have three crystals, each one of them irradiated in different conditions, with almost exactly the same $\alpha_{SP}(l_D) \approx 3.4^\circ$. One of them shows a clear matching effect (A1, see Fig. 1); another one shows just a minor hint [B3, Fig. 4(c)]; and the third one shows no effect (C1, Fig. 3).

Figure 5 shows that, using a single parameter, we have been able to ascertain under what conditions matching effects are observable in YBCO with CD. We do not claim that $\alpha_{SP}(l_D)$ is the only or even the best quantifier of the tracks disorder; it is just a simple, reasonable and convenient one. An implicit assumption, for instance, is that splay and pinning energy dispersion are strongly correlated and thus can be characterized by a single number. A more elaborated analysis could produce a better quantifier, but we should emphasize that our description successfully describes the behavior of our 14 crystals and all the films of Ref. 6, with no exceptions.

C. Relaxation studies

We have observed the maximum at H_m in temperatures ranging from $40K$ up to as high as $80K$, very close to the irreversibility line.¹⁶ This result is somewhat surprising, since the Mott phase is only expected at low T .^{1,2} It is true that the broad peak in $M_i(H)$ seen in our crystals and in the films of Ref. 6 (where it was described as a *vestige* of the Mott phase) is a feature far less dramatic than the Meissner-like response of the Mott insulator. But on the other hand, the physical origin is clearly the same: The maximum in the pinning efficiency of the CD at $B \sim B_\Phi$ occurs because, being all the vortices pinned and all the tracks occupied, there are no energetically convenient places for a vortex to move on from its initial

position.

If the above picture is correct, the maximum in $M_i(H)$ should be accompanied by a decrease of the creep rate. This is precisely the feature used by Beauchamp *et al.*⁴ and by Nowak *et al.*⁵ to identify the Mott insulator phase at very low T . Fig. 1(b) shows the normalized relaxation rate S as a function of $\mathbf{H} \parallel \text{CD}$ at $T = 60K$ for crystal A1. For $H \sim B_\Phi$ a local minimum appears, thus confirming that matching fields effects at these high temperatures are due to a reduction of the creep processes.

It is important to realize that in the temperature range of our observations the vortex system is in the collective pinning regime.³ Crystal B1 is the same one investigated in Ref. 3. It was shown there that the *accommodation field* $B_a(T)$ (the boundary between individual and collective pinning) goes to zero at the *depinning temperature* $T_{dp} \approx 40K$, thus for $T > T_{dp}$ the pinning is collective for all values of H . The abrupt collapse of $B_a(T)$ at $T_{dp} \approx 40K$ was observed not only in B1 but also in all the other crystals reported there (irradiated in all cases with $1.08GeV Au^{23+}$), regardless of B_Φ . Recent results¹⁷ indicate that T_{dp} for crystals irradiated with $580MeV Sn^{30+}$ and $300MeV Au^{24+}$ is also very similar.

To our knowledge, a determination of $B_a(T)$ for tracks' orientations other than the c -axis was not available. Thus, to check whether the large Θ_D makes any difference in this respect, we determined $B_a(T)$ for crystal A1. To that end we measured the normalized relaxation rate S as a function of T at several $\mathbf{H} \parallel \text{CD}$, as shown in the inset of Fig. 2. The maxima in these curves, which indicate the onset of the collective pinning regime, have been used³ as a signature of $B_a(T)$. The collective regime becomes completely developed when $S(T)$ reaches the *plateau* at higher temperatures.^{8,17} The temperature range in between the maxima and the *plateau* (i.e., the region where S decreases with T) is a transition zone where individual and collective excitations coexist.¹⁷ The *accommodation field* and the transition zone are included in the complete dynamic phase diagram shown in the main frame of Fig. 2. This diagram again shows that $T_{dp} \approx 35K$, and it clearly demonstrates that also in crystal A1 the vestiges of the Mott insulator phase (the $H_m(T)$ line) lie well inside the collective pinning regime.

Within this regime and at fixed T , the critical current should have a $1/H$ dependence.^{1,2} Therefore, a monotonically increasing $S(H)$ is also expected. This is indeed the observed behavior in Fig. 1(b), with the local minimum at B_Φ mounted on the increasing curve. This feature once again shows the presence of the matching effects in the collective pinning regime.

IV. DISCUSSION

A. Dispersion-induced slow-down of creep

The two main results of our study are that matching effects occur deep into the collective pinning regime, and that these effects are destroyed by sufficiently large splay and dispersion of pinning energy in the system of CD. We will now discuss the second result, and in the next subsection we will address the first one.

According to the theoretical models,^{1,2} the main features of the pinning diagram are expected to be robust with respect to the energy dispersion and splay: Pinning by CD in HTSC should still be individual and strong at low T and H , and should become collective and weaker above $B_a(T)$, as either T or H increase. Experimental results confirm that expectation,^{3,8,11,17} as the basic pinning behavior is similar in all samples, in spite of the fact that they contain different amounts of dispersion in the CD system. In contrast, the dynamic at current densities well below J_c is strongly influenced by the dispersion in the CD.^{10,17} This indicates that the link between the amount of dispersion in the CD and the observation of matching effects must be related to the influence of the dispersion on the creep processes.

In the single vortex pinning regime, time relaxation at the early stages takes place^{1,2} via nucleation and expansion of *half loops*. As J decreases the size of the critical nucleus grows and eventually reaches the nearest CD. Further relaxation proceeds by spreading of the resulting *double kink* vortex excitations. Ideally, if energy dispersion and splay are not taken into account, there is no barrier for the expansion of a double kink critical nucleus, and J should decrease very rapidly.^{1,2} In the collective pinning regime the creep mechanisms are somewhat different and less explored theoretically. However, vortex bundles are also expected to relax via collective double kinks,² whose expansion is again unimpeded in the absence of splay and energy dispersion.

Both splay and energy dispersion of the CD will arrest the expansion of double kinks, since both reduce the number of sites with equivalent energy available for the hopping and spreading processes. As a result, the J determined from magnetization measurements is larger than it should be in the absence of dispersion. The idea of topological constraints on vortex hopping was first discussed by Hwa *et al.*¹⁸ It is indeed established experimentally¹⁹ that a certain amount of splay enhances M_i in YBCO. In particular, by comparing YBCO crystals of different thicknesses, irradiated with different ions and energies, it has been shown that the splay reduces the creep rate.¹⁰

Energy dispersion makes the expansion of double kinks energetically unfavorable in the limit $J \rightarrow 0$.^{1,2} Double kink excitations are then substituted by *superkinks*, whose associated time relaxation (the so called *variable range hopping* regime) is much slower. We have recently demonstrated¹⁷ that fast relaxation by double kinks does occur in YBCO crystals, and that the crossover to the superkinks regime and the associated slow-down of the

creep takes place at a current density J_{VRH} which is proportional to the energy dispersion.

The above discussion leads us to propose the following scenario. In those samples where splay and energy dispersion are small, time relaxation is fast and the overall measured M_i is low. However, near the matching condition creep slows down due to the absence of available sites. As a result, the M_i measured at a given time is higher around B_Φ than in the rest of the field range, thus producing the observed maximum. In contrast, the large amount of splay and energy dispersion in thick samples limits the expansion of double kinks at all fields. As a consequence, the creep rate becomes lower in the whole field range, and the creep reduction near B_Φ becomes negligible or entirely absent. In these conditions, the overall M_i is high and the distinct maximum at the matching condition disappears.

Finally, the weak decrease of H_m with temperature could be related to the small but nonzero dispersion of pinning energies. The effectiveness of the CD is strongly reduced with increasing T due to the entropic smearing.³ Therefore, some weak CD can pin vortices at low temperatures but cannot hold them pinned at high T , thus slightly reducing the effective matching field.

B. Matching effects in the collective pinning regime

Previous numerical simulations²⁰ of matching effects within the collective pinning regime have been able to predict some effects of the Mott phase at high temperatures, but only in the case $\lambda/d \leq 1$, where λ is the penetration length and $d = \sqrt{\Phi_0/B_\Phi}$ the average distance between CD. This inequality results from the condition that the vortex-vortex interactions have to be of short range as compared with the distance between tracks (that equals the distance between flux lines at $B = B_\Phi$). However, in our case $\lambda \approx 1400\text{\AA}$ and d ranges from 190\AA for crystal B2 to 300\AA for crystal A1, which gives $\lambda/d \geq 4.7$ in all cases.

Krauth *et al.*²¹ have studied the problem of 2D bosons in a disordered environment, which is analogous to the problem of flux lines in the presence of CD.¹ Through Monte Carlo numerical simulations they have found that the Mott insulator phase could be present up to the transition to the Bose glass phase. But again, they have used only on-site repulsion, which is equivalent to the condition $\lambda/d < 1$, i.e., negligible vortex-vortex interactions.

More recently, Sugano *et al.*²² have performed Monte Carlo numerical simulations of pancake vortices in the much more anisotropic $\text{Bi}_2\text{Sr}_2\text{CaCu}_2\text{O}_8$ system, with CD parallel to the c -axis. Neither splay nor pinning energy dispersion were considered. The main result of that study is the observation of a field-driven discontinuous transition in the trapping rate of the pancakes to the CD, at a field $\sim B_\Phi/3$, that is accompanied by a large jump in the interlayer coherence. This result is in agreement with

recent Josephson Plasma resonance experiments²³ and c -axis resistivity measurements²⁴ in the liquid phase, and is also consistent with several experimental observations of anomalies in the solid phase.²⁵ Similarly, anomalies in H_{irr} and maxima in $M_i(H)$ have been observed^{11,16} in the YBCO system, in the field range $\sim B_\Phi/3$ to $\sim B_\Phi/2$. An additional result of these simulations, particularly relevant to our present work, is the observation²² of a high temperature "subanomaly" at the matching field $\sim B_\Phi$, thought to be a *remnant* of the low-temperature Mott insulator phase. This subanomaly is accompanied by a sudden increase in the vortex trapping rate, i.e., a slow down of creep, which according to those simulations is dominated by expansion of *double kinks*. All these results are consistent with our scenario, according to which the maximum in $M_i(H)$ at $H \sim B_\Phi$ is due to the reduction of the rate of creep by double kink excitations. Topological vortex entanglement, forced by splay present in the thicker crystals, as well as large pinning energy dispersion, erase this matching subanomaly by constraining the expansion of double kinks at all fields.

V. CONCLUSIONS

We have observed matching field effects in the irreversible magnetization and its time relaxation in $\text{YBa}_2\text{Cu}_3\text{O}_7$ single crystals with columnar defects. We have demonstrated that a necessary condition for the appearance of these effects is a low level of angular and energy dispersion in the CD system. To achieve this situation, an adequate combination of thin samples and high irradiation energy is required. Large dispersion precludes the appearance of matching effects by slowing down the creep processes over the whole field range. We propose the value of the splay at the back face of the sample, $\alpha_{SP}(l_D)$, as a convenient parameter to quantify the dispersion. Surprisingly, these matching effects are observed at high temperatures, deep into the collective pinning regime, where the Mott phase is not expected.

ACKNOWLEDGMENTS

This work was partially supported by ANPCyT, Argentina, PICT 97 No. 01120. A.S. and G.N. would like to thank the CONICET for financial support.

¹ D. R. Nelson and V. M. Vinokur, Phys. Rev. B **48**, 13060 (1993).

² G. Blatter, M. V. Feigel'man, V. B. Geshkenbein, A.I. Larkin, and V. M. Vinokur, Rev. Mod. Phys. **66**, 1125 (1994).

³ L. Krusin-Elbaum, L. Civale, J. R. Thompson, and C. Feild, Phys. Rev. B **53**, 11744 (1996).

- ⁴ K. M. Beauchamp, T. F. Rosenbaum, U. Welp, G. W. Crabtree, and V. M. Vinokur, Phys. Rev. Lett. **75**, 3942 (1995).
- ⁵ E. R. Nowak, S. Anders, H. M. Jaeger, J. A. Fendrich, W. K. Kwok, R. Mogilevsky, and D. G. Hinks, Phys. Rev. B **54**, 12725 (1996).
- ⁶ A. Mazilu, H. Safar, M. P. Maley, J. Y. Coulter, L. N. Bulaevskii, and S. Foltyn, Phys. Rev. B **58**, 8909 (1998).
- ⁷ F. de la Cruz, D. López, and G. Nieva, Philos. Mag. B **70**, 773 (1994).
- ⁸ L. Civale, G. Pasquini, P. Levy, G. Nieva, D. Casa, and H. Lanza, Physica C **263**, 389 (1996).
- ⁹ F. Holtzberg and C. Feild, Eur. J. Solid State Inorg. Chem. **27**, 107 (1990).
- ¹⁰ L. Civale, L. Krusin-Elbaum, J. R. Thompson, R. Wheeler, A. D. Marwick, M. A. Kirk, Y. R. Sun, F. Holtzberg, and C. Feild, Phys. Rev. B **50**, 4102 (1994).
- ¹¹ L. Civale, A. D. Marwick, T. K. Worthington, M. A. Kirk, J. R. Thompson, L. Krusin-Elbaum, Y. Sun, J. R. Clem, and F. Holtzberg, Phys. Rev. Lett. **67**, 648 (1991).
- ¹² A. Silhanek, L. Civale, S. Candia, G. Nieva, G. Pasquini, and H. Lanza, Phys. Rev. B **59**, 13620 (1999).
- ¹³ E. H. Brandt, Phys. Rev. B **49**, 9024 (1994); J. R. Clem and A. Sanchez, *ibid* **50**, 9355 (1994).
- ¹⁴ See for example F. Studer and M. Toulemonde, Nucl. Instr. Meth. B **65**, 560 (1992); V. Hardy *et al.*, *ibid* **54**, 472 (1991); A. D. Marwick *et al.*, Proceedings of the Eighth International Conference on Ion Beam Modification of Materials (1992); D. X. Huang *et al.*, Phys. Rev. B **57**, 13907 (1998).
- ¹⁵ R. Wheeler, M. A. Kirk, R. Brown, A. D. Marwick, L. Civale, and F. Holtzberg, in Phase Formation and Modification by Beam-Solid Interactions, edited by G. S. Was, L. E. Rehn, and D. M. Follstaedt (MRS Symposium Proceedings - Vol. 235, Pittsburgh, 1992), p. 683.
- ¹⁶ L. Krusin-Elbaum, L. Civale, G. Blatter, A. D. Marwick, F. Holtzberg, and C. Feild, Phys. Rev. Lett. **72**, 1914 (1994).
- ¹⁷ D. Niebieskikwiat, L. Civale, C. A. Balseiro, and G. Nieva, Phys. Rev. B **61**, 7135 (2000).
- ¹⁸ T. Hwa, P. Le Doussal, D. R. Nelson, and V. M. Vinokur, Phys. Rev. Lett. **71**, 3545 (1993).
- ¹⁹ L. Krusin-Elbaum, A. D. Marwick, R. Wheeler, C. Feild, V. M. Vinokur, G. K. Leaf, and M. Palumbo, Phys. Rev. Lett. **76**, 2563 (1996).
- ²⁰ C. Wengel and U. C. Täuber, Phys. Rev. B **58**, 6565 (1998).
- ²¹ W. Krauth, T. Trivedi, and D. Ceperley, Phys. Rev. Lett. **67**, 2307 (1991).
- ²² R. Sugano, T. Onogi, K. Hirata, and M. Tachiki, Phys. Rev. Lett. **80**, 2925 (1998).
- ²³ Sato *et al.*, Phys. Rev. Lett. **79**, 3759 (1997); Kosugi *et al.*, *ibid* **79**, 3763 (1997); Tsuchiya *et al.*, Phys. Rev. B **59**, 11568 (1999).
- ²⁴ N. Morozov *et al.*, Phys. Rev. B **57**, R8146 (1998); Phys. Rev. Lett. **82**, 1008 (1999).
- ²⁵ N. Chikumoto *et al.*, Phys. Rev. B **57**, 14507 (1998); C. J. Van der Beek *et al.*, *ibid* **61**, 4259 (2000); K. Itaka *et al.*, preprint (2000).

FIG. 1. (a) Curves of irreversible magnetization M_i vs applied field H for crystal A1 at several temperatures for $\mathbf{H} \parallel \text{CD}$. The dotted line is a guide to the eye indicating

the position of the maximum $H_m(T)$. (b) Normalized relaxation rate as a function of H at $T = 60\text{K}$. The local minimum is generated by the reduction of the mobility of the flux lines when $H \sim B_\Phi$.

FIG. 2. Dynamic H - T phase diagram for crystal A1. The solid triangles represent the accommodation field $B_a(T)$. The solid circles indicate the line $H_m(T)/B_\Phi$. For comparison, the $H_m(T)/B_\Phi$ data for a thick film of Ref. 6 is also shown (open circles). Inset: Normalized relaxation rate $S(T)$ curves at several fields. The maximum indicates the onset of the collective excitations at high T .

FIG. 3. Irreversible magnetization M_i as a function of H/B_Φ for several crystals at $T = 60\text{K}$ and $\mathbf{H} \parallel \text{CD}$. None of these samples show any hint of matching effects at $H \sim B_\Phi$.

FIG. 4. Irreversible magnetization as a function of H at several T for three crystals that exhibit matching effects. For clarity, some curves are multiplied by a numerical factor, as indicated.

FIG. 5. Median radial angle α_{SP} of the CD at the back face of the sample as a function of the total tracks' length l_D . Samples with $\alpha_{SP}(l_D) < 3.4^\circ$ exhibit matching effects, as opposed to the crystals with $\alpha_{SP}(l_D) > 3.4^\circ$.

TABLE I. Irradiation and thickness specifications for all the crystals studied. The crystals labeled with an asterisk present matching effects.

Crystal	ion	$B_{\Phi}(T)$	Θ_D	$\delta(\mu m)$	$\delta / \cos \Theta_D(\mu m)$
A1*	300MeV Au ²⁴⁺	2.2	57°	4.1	7.5
A2	300MeV Au ²⁴⁺	3.7	15°	8.2	8.5
A3	300MeV Au ²⁴⁺	3.0	32°	8.5	10.0
B1*	1080MeV Au ²³⁺	4.7	0°	11.5	11.5
B2*	1080MeV Au ²³⁺	5.7	30°	11.5	13.3
B3*	1080MeV Au ²³⁺	2.4	0°	24.7	24.7
B4	1080MeV Au ²³⁺	0.6	0°	26.8	26.8
B5	1080MeV Au ²³⁺	1.0	65°	11.4	27.0
B6	1080MeV Au ²³⁺	1.1	2°	31.0	31.0
C1	580MeV Sn ³⁰⁺	1.0	2°	20.5	20.5
C2	580MeV Sn ³⁰⁺	3.0	2°	22.0	22.0
C3	580MeV Sn ³⁰⁺	3.0	30°	20.9	24.1
C4	580MeV Sn ³⁰⁺	3.0	2°	25.7	25.7
C5	580MeV Sn ³⁰⁺	5.0	2°	27.0	27.0

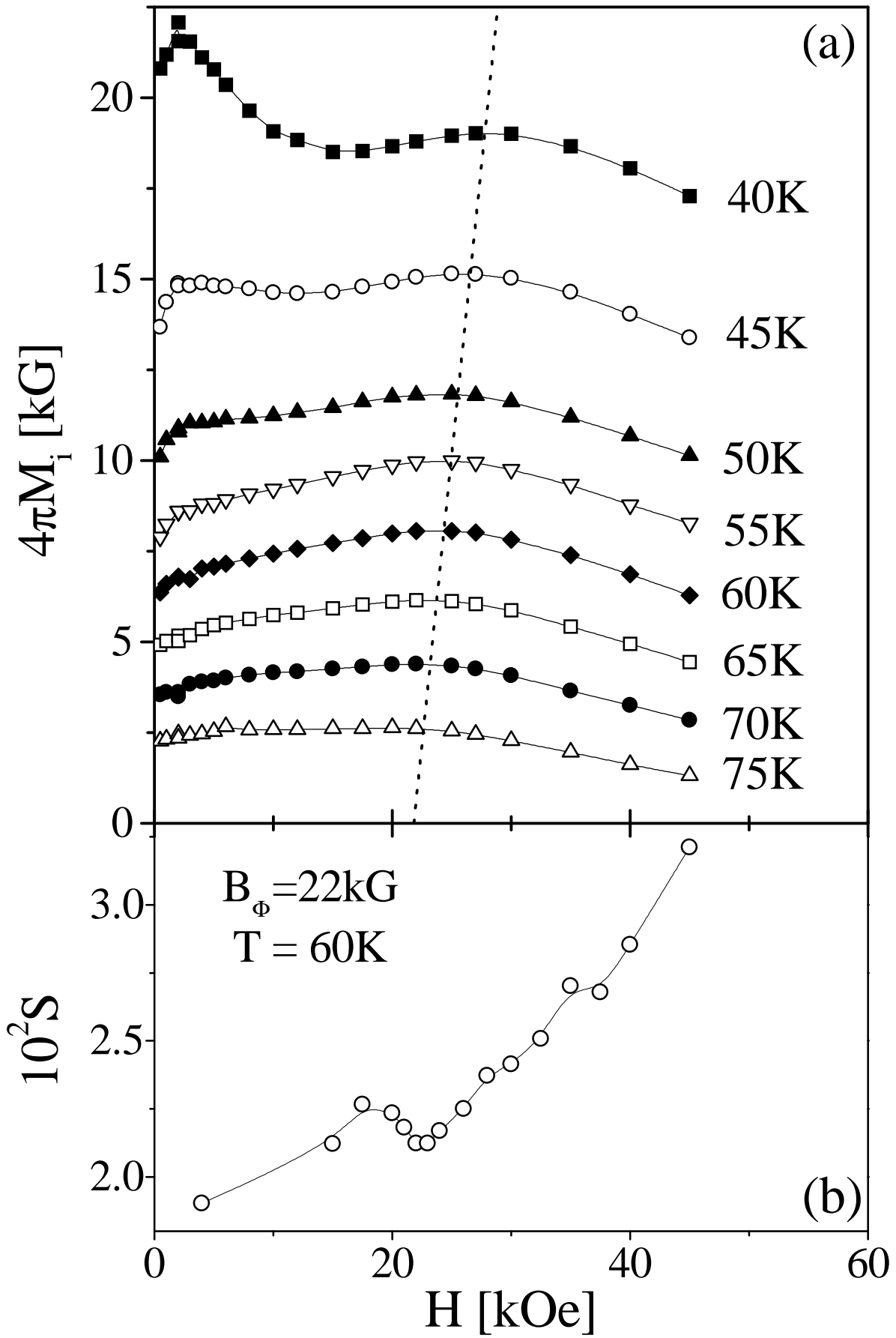


Figure 1

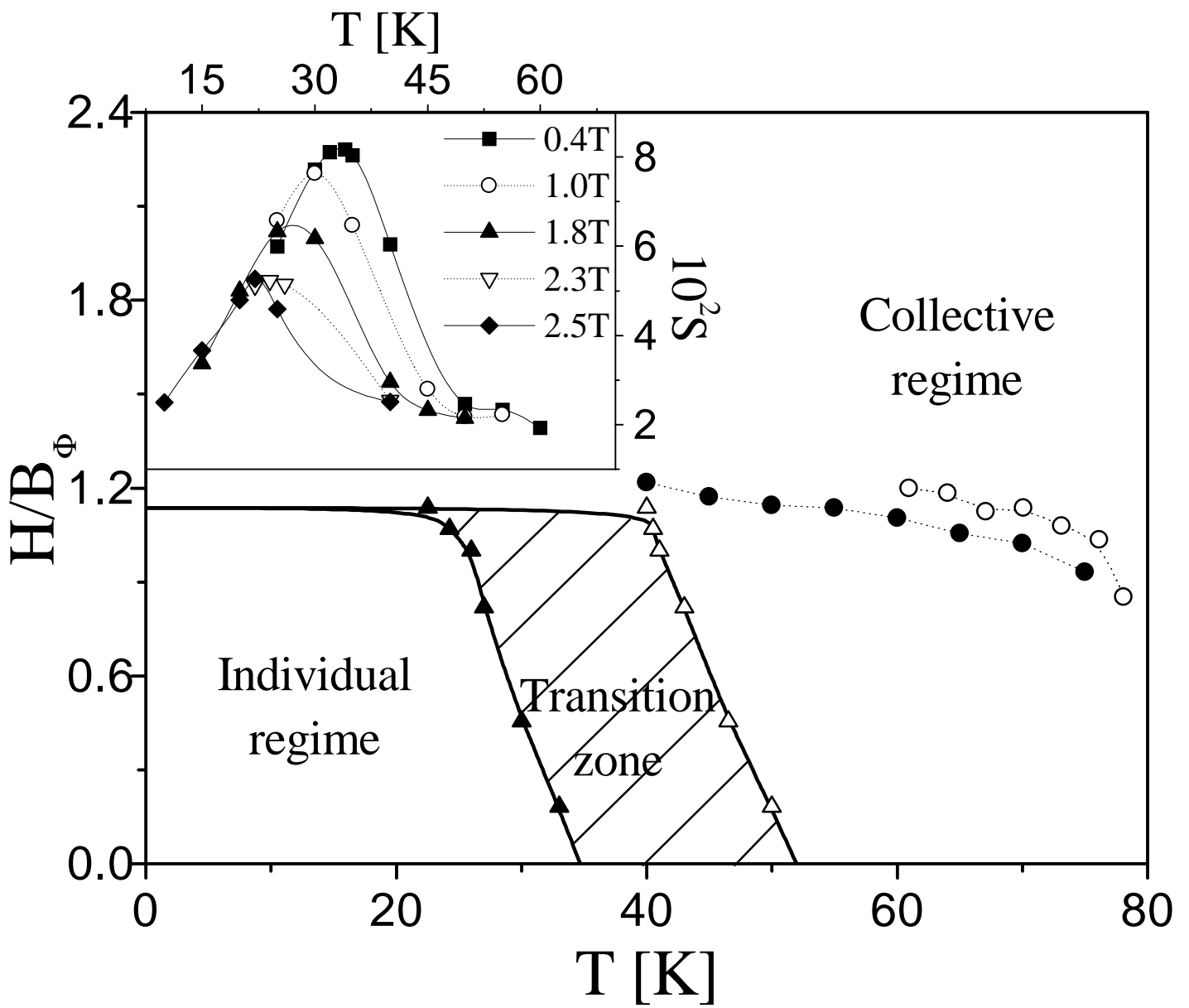


Figure 2

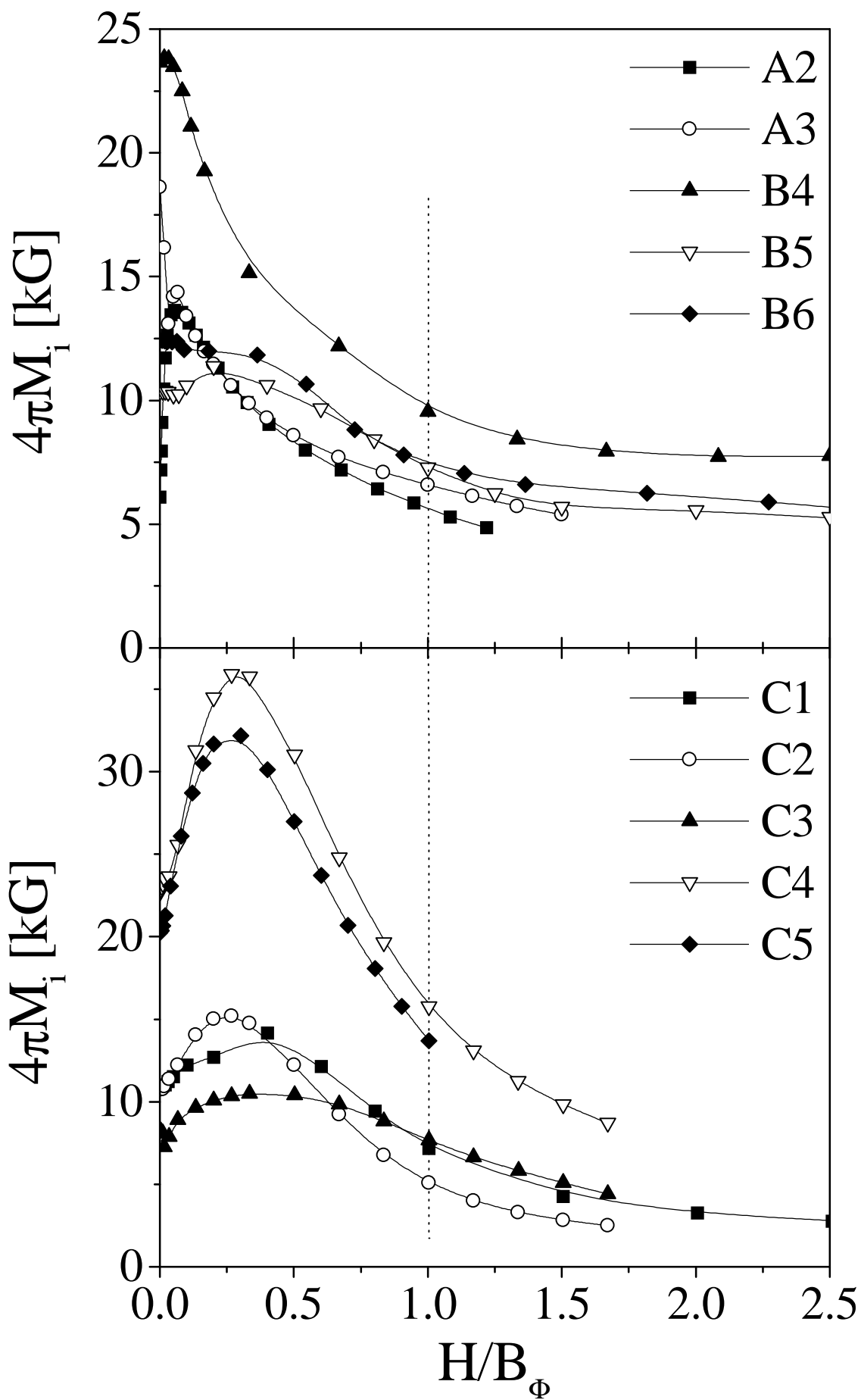


Figure 3

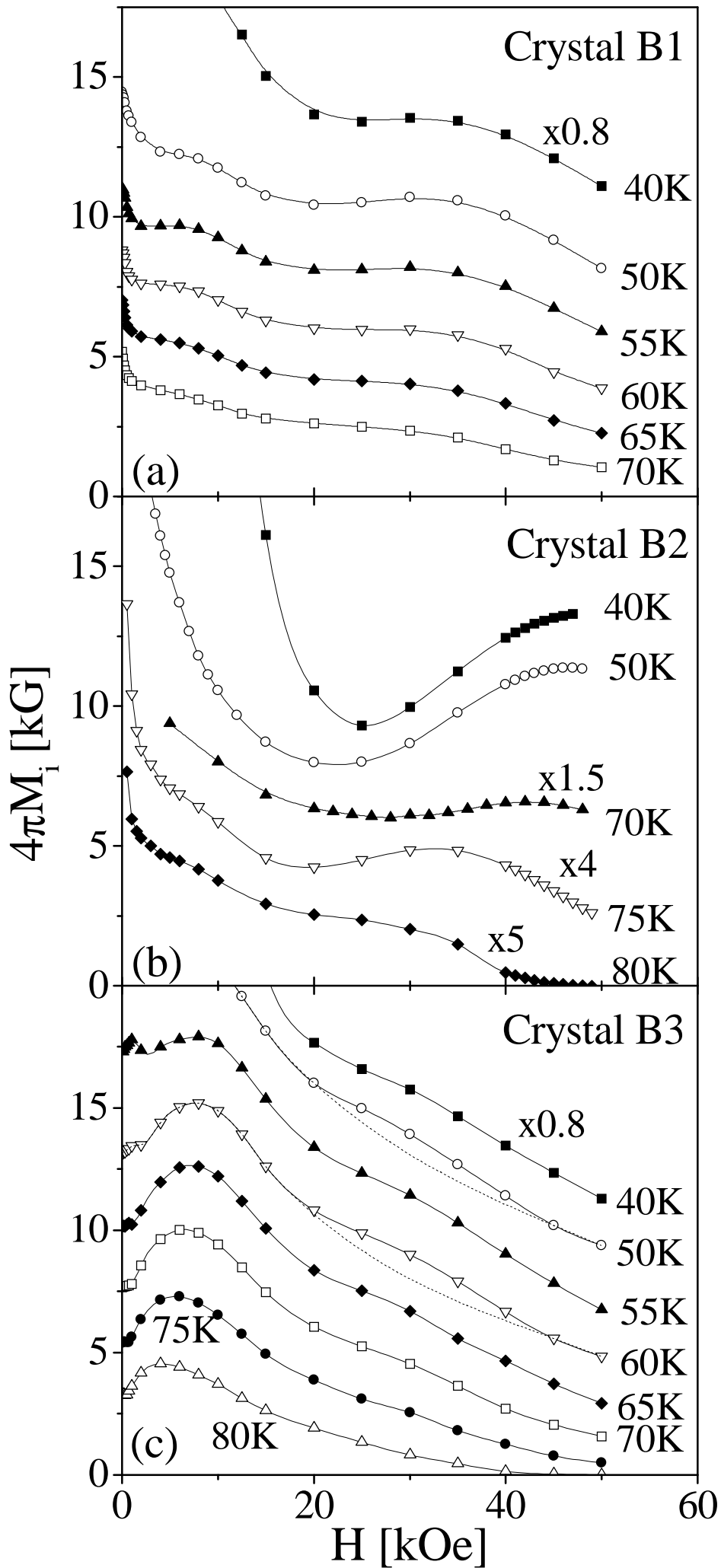


FIGURE 4

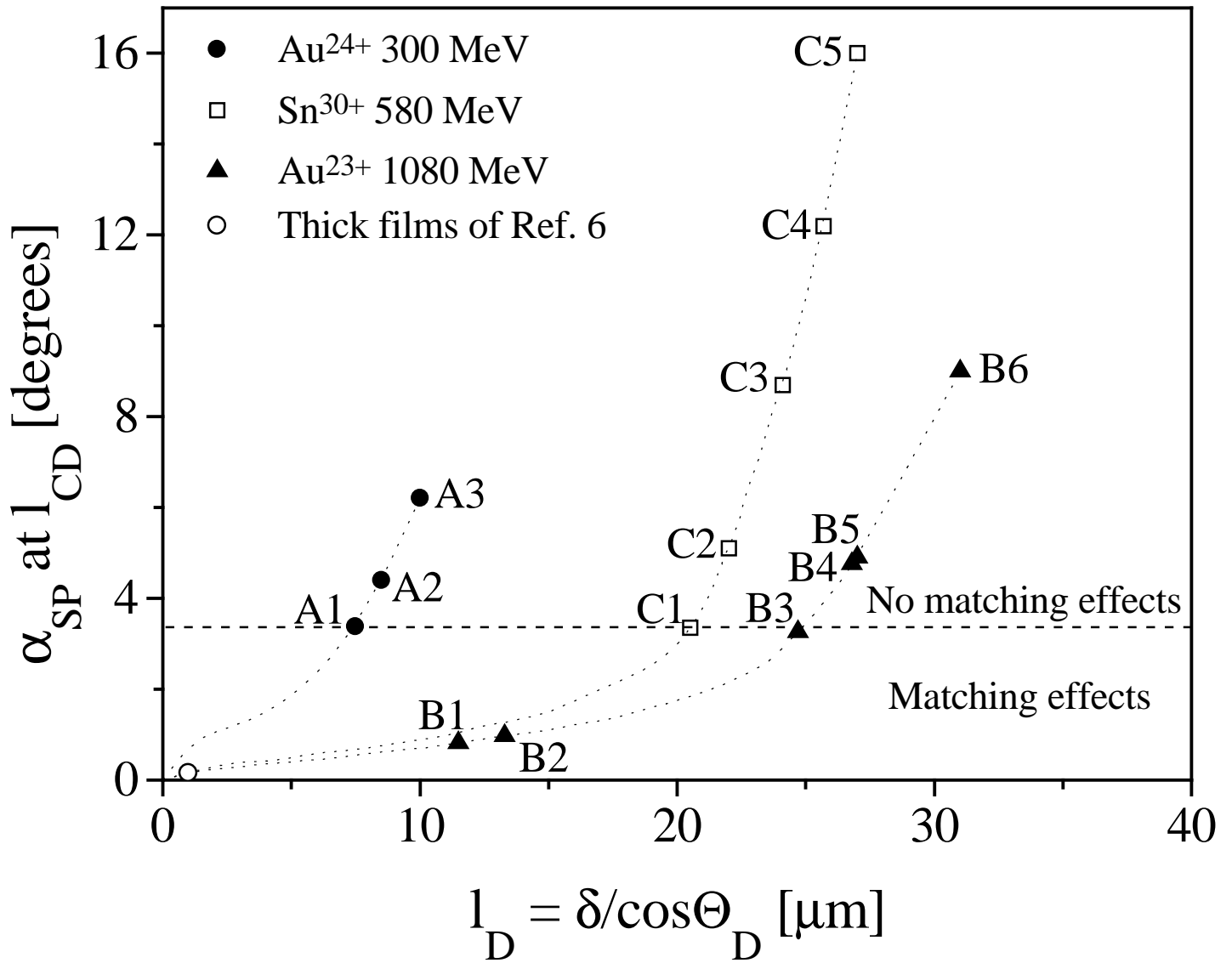


Figure 5